Special Section on Transporters in Drug Disposition and Pharmacokinetic Prediction

Liver Zonation Index of Drug Transporter and Metabolizing Enzyme Protein Expressions in Mouse Liver Acinus [S]

Masanori Tachikawa, Yuna Sumiyoshiya, Daisuke Saigusa, Kazunari Sasaki, Michitoshi Watanabe, Yasuo Uchida, and Tetsuya Terasaki

Membrane Transport and Drug Targeting Laboratory, Graduate School of Pharmaceutical Sciences (M.T., Y.S., K.S., M.W., Y.U., T.T.), and Department of Integrative Genomics, Tohoku Medical Megabank Organization (D.S.), Tohoku University, Sendai, Japan

ABSTRACT

The purpose of the present study was to clarify the molecular basis of zonated drug distributions in mouse liver based on the protein expression levels of transporters and metabolizing enzymes in periportal (PP) and pericentral (PC) vein regions of mouse hepatic lobules. The distributions of sulforhodamine 101 (SR-101), a substrate of organic anion transporting polypeptides (Oatps), and ribavirin, a substrate of equilibrative nucleoside transporter 1 (Ent1), were elucidated in frozen liver sections of mice, to which each compound had been intravenously administered. Regions strongly positive for SR-101 (SR-101$^+$) and regions weakly positive or negative for SR-101 (SR-101$^-$) were separated by laser microdissection. The zonated distribution of protein expression was quantified in terms of the liver zonation index. Quantitative targeted absolute proteomics revealed the selective expression of glutamine synthetase in the SR-101$^+$ region, indicating predominant distribution of SR-101 in hepatocytes of the PC vein region. The protein levels of Oatp1a1, Oatp1b2, organic cation transporter 1 (Oct1), and cytochrome P450 (P450) 2e1 were greater in the PC vein regions, whereas the level of organic anion transporter 2 (Oat2) was greater in the PP vein regions. Mouse Oatp1a1 mediated SR-101 transport. On the other hand, there were no statistically significant differences in expression of Ent1, Na$^+$-taurocholate cotransporting polypeptide, several canalicular transporters, P450 enzymes, and UDP-glucuronosyltransferases between the PP and PC vein regions. This is consistent with the almost uniform distribution of ribavirin in the liver. In conclusion, sinusoidal membrane transporters such as Oatp1a1, Oatp1b2, Oct1, and Oat2 appear to be determinants of the zonated distribution of drugs in the liver.

Introduction

Transport and metabolism in hepatocytes are key determinants of drug whole-body clearance, as well as drug efficacy in the liver as a target organ. Therefore, during drug development hepatic drug transport and metabolizing activities are generally evaluated by using primary-cultured or freshly isolated human hepatocytes, as well as whole-liver homogenate and in vivo rodent and monkey studies (Houston et al., 2012; Godoy et al., 2013). Analysis is often based on the approximation of a well-stirred model, employing the assumption that hepatocytes exhibit uniform drug transport and metabolism activities throughout the liver. However, the concept of liver metabolic zonation is long established, i.e., xenobiotic metabolism is predominant in hepatocytes

around the pericentral (PC) vein, whereas oxidative energy metabolism, gluconeogenesis, urea synthesis, and bile formation are catalyzed mainly in hepatocytes around the periportal (PP) vein (Katz, 1992). Furthermore, protein expression and metabolizing activity of cytochrome P450s such as CYP2A, 2B, 2E, and 3A, are predominantly seen in PC vein hepatocytes (Oinonen and Lindros, 1998). Indeed, recent studies with imaging mass spectrometry have confirmed the spatial heterogeneity of drug disposition and metabolism in the liver (Takai and Tanaka, 2015). These lines of evidence suggest that PP and PC vein hepatocytes differ in their capacity for drug metabolism and transport in the liver acinus. Therefore, our aim was to clarify the molecular basis of the spatial heterogeneity and functional zonation to achieve better understanding of drug targeting to the liver, hepatic clearance, and drug-drug interaction.

Biliary excretion through hepatocytes is an essential process in hepatic drug disposition. It involves 1) uptake mediated by solute carrier transporters on the sinusoidal membrane; 2) sequential metabolism mediated by various metabolizing enzymes, such as cytochrome P450,

ABBREVIATIONS: Ent1, equilibrative nucleoside transporter 1; LC-MS/MS, liquid chromatography–tandem mass spectrometry; LMD, laser microdissection; Mrp, multidrug resistance-associated protein; Oat2, organic anion transporter 2; Oatp, organic anion transporting polypeptide; Oct1, organic cation transporter 1; PC, pericentral; PP, periportal; QTAP, quantitative targeted absolute proteomics; SR-101, sulforhodamine 101; SRM, selective reaction monitoring.

uridine diphosphate-glucuronosyltransferase, and sulfotransferase; and 3) excretion mediated by ATP-binding cassette transporters on the bile canalicular membranes. It is considered that PP vein hepatocytes play a predominant role in the uptake and the biliary excretion of bile acids and organic anions under physiologic conditions (Gumucio et al., 1978; Jones et al., 1980; Groothuis et al., 1982). However, on the other hand, the biliary excretion of temocaprilat and pravastatin is markedly decreased specifically by injury to the PC vein region, whereas the biliary excretion of bromosulphophthalein and leukotriene C_4 is markedly decreased specifically by injury to the PP vein region in rats (Aiso et al., 2000; Takikawa et al., 2001; Sasamoto et al., 2006). Temocaprilat and pravastatin are substrates of organic anion transporting polypeptide (Oatp)1a1 and Oatp1a4, respectively (Ishizuka et al., 1998; Tokui et al., 1999), although in addition, temocaprilat (Ishizuka et al., 1997), pravastatin (Ellis et al., 2013), bromosulphophthalein, and leukotriene C_4 (Ninomiya et al., 2006) are all substrates of multidrug resistance-associated protein (Mrp) 2 (Mrp2) in rats. These results imply that the zone-predominant expression of transporters, e.g., Oatps in PC vein hepatocytes, may play a key role in the sinusoidal uptake of temocaprilat and pravastatin.

Quantitative targeted absolute proteomics (QTAP)–based protein quantification has enabled us to determine the absolute protein expression levels of transporters and metabolizing enzymes in the livers of humans and mice (Kamiie et al., 2008; Kawakami et al., 2011; Ohtsuki et al., 2011, 2012). Our previous analyses with QTAP have demonstrated the lack of correlation between mRNA and protein amounts of the plasma membrane transporters in human liver (Ohtsuki et al., 2012), but a good correlation was found between the protein amounts of organic cation/carnitine transporter 1 and MRP1 and their transport activities in primary cultured human respiratory epithelial cells (Sakamoto et al., 2016). Furthermore, most of the work on metabolic zonation has been done at the transcriptional level by using reverse transcription polymerase chain reaction and at the protein level by immunohistochemical analysis, in which there have been conflicting results, for example, regarding the regional expression of Mrp2 (Baier et al., 2006; Micuda et al., 2008). We considered that the QTAP strategy would be the most suitable approach to establish the functional contribution of transporters and enzymes to drug metabolism and transport in PP and PC vein hepatocytes. Thus, the purpose of the present study was to clarify the molecular basis of region-predominant transport and/or metabolism in the liver based on the protein expression levels of transporters and enzymes in the PP and PC vein regions of mouse liver lobule as determined by laser microdissection (LMD)–based zone-specific sampling and QTAP-based protein quantification.

Material and Methods

Materials. Methanol and acetonitrile were purchased from Kanto Chemical (Tokyo, Japan). Formic acid and ribavirin were purchased from Wako Pure Chemical Industries (Osaka, Japan). Sulforhodamine 101 (SR-101) and $^{13}C_6$-arginine were purchased from Sigma-Aldrich (Tokyo, Japan).

Sample Preparation by LMD for Liquid Chromatography Tandem–Mass Spectrometry (LC-MS/MS) Analysis. Adult male ddY mice (7–11 weeks old) were purchased from SLC Japan (Shizuoka, Japan). The mice were maintained on a 12-hour light/dark cycle in a temperature-controlled environment with free access to food and water. All experiments were approved by the Institutional Animal Care and Use Committee at Tohoku University, and performed in accordance with guidelines at Tohoku University. Under deep anesthesia with isoflurane, the fluorescent dye SR-101 (a known substrate of Oatps) (40 mg/kg wt.) or ribavirin (200 mg/kg wt.) was intravenously administered to the mice. Then, 30 or 90 minutes after administration, the mice were transcardially perfused for 2 to 3 seconds with phosphate-buffered saline to remove the circulating blood in the liver. It has been demonstrated that biliary excretions of organic anions, e.g., taurochenodeoxycholate-3-sulfate and

pravastatin are maximal at 15–20 minutes after a bolus injection into the rat femoral vein (Sasamoto et al., 2006). To examine regional differences in the total hepatobiliary transport process of sinusoidal uptake followed by biliary excretion of SR-101 or ribavirin after a bolus intravenous injection, the time points of 30 and 90 minutes were chosen. The mouse liver tissues were freshly obtained and immediately frozen in powdered dry ice. Frozen sections (20 μm in thickness) were prepared on a cryostat (CM1900; Leica, Nussloch, Germany), mounted on LMD slides (DIRECTOR; Expression Pathology, Gaithersburg, MD), and air dried. Regions strongly positive for SR-101 (SR-101$^+$) and regions weakly positive or negative for SR-101 (SR-101$^-$) with a total area of 5 mm^2 for ribavirin and SR-101 quantification or 25 mm^2 for protein quantification were identified under fluorescent light and collected by LMD using a Leica device (LMD6500; Leica). Three independent mice were used to obtain each SR-101$^+$ and SR-101$^-$ regions of liver tissues. The microdissected tissues were placed in 0.5 ml microcentrifuge tubes.

LC-MS/MS Quantification of SR-101 and Ribavirin in Microdissected Tissues. The microdissected tissues were homogenized with 50 μl of methanol containing 0.1% formic acid and $^{13}C_6$-arginine (internal standard) in an ultrasonic bath for 10 minutes and centrifuged at 16,400g for 10 minutes at 4°C. For ribavirin quantification, the supernatant was evaporated in a CC-105 centrifugal concentrator (low heat mode; Tomy, Tokyo, Japan) for 1 hour, and the residue was reconstituted in ammonium acetate buffer (pH 4.8). The solution was incubated with 50 mU acid phosphatase (Sigma-Aldrich) at 37°C for 1 hour for dephosphorylation of ribavirin phosphate and centrifuged in methanol containing 0.1% formic acid for enzymatic protein. The supernatant was analyzed by LC-MS/MS. The LC-MS/MS system consisted of a NANOSPACE SI-II HPLC, equipped with a dual pump system, an autosampler, and a column oven (Shiseido, Tokyo, Japan), together with a TSQ Quantum Ultra triple quadrupole mass spectrometer (Thermo Fisher Scientific, San Jose, CA) equipped with a HESI-II source. Quantification analyses were performed in the selective reaction monitoring (SRM) mode. The transitions of the precursor ion to the product ion, tube lens voltage (in volts), and collision energy (in electron volts) were as follows: m/z 245 → 96, 104 V, and 31 eV for ribavirin; m/z 604.9 → 525.3, 180 V, and 42 eV for SR-101; and m/z 181 → 74, 83 V, and 21 eV for $^{13}C_6$-arginine with a cycle time of 0.5 seconds. The optimized parameters for mass spectrometry were as follows: spray voltage for positive ion mode and negative ion mode, 3.0 and 2.5 kV, respectively; heated capillary temperature, 220°C; sheath gas pressure, 50 psi; auxiliary gas setting, 15 psi; and heated vaporizer temperature, 200°C. The sheath and auxiliary gases were nitrogen. The collision gas was argon at a pressure of 1.5 mTorr. Liquid chromatography separation was performed using a normal-phase (hydrophilic interaction chromatography) column (ZIC^R-hydrophilic interaction chromatography; 100 × 2.1 mm i.d., 3.5 μm particle size; Sequant, Darmstadt, Germany) with a gradient of solvent A (water containing 0.1% formic acid) and solvent B (acetonitrile containing 0.1% formic acid) at 0.2 ml min^{-1}. The initial condition was set at 100% B, linearly decreasing to 20% B from 2 to 4 minutes, and maintained at 100% B for 3 minutes. Subsequently, the mobile phase was immediately returned to the initial conditions and maintained for 5 minutes until the end of the run. The total run time was 12 minutes for the analysis and the oven temperature was 40°C. The LC-MS/MS system was controlled and analyzed using Xcalibur software (Thermo Fisher Scientific).

LC-MS/MS-Based Protein Quantification of Transporters/Receptors and Enzymes in Microdissected Liver Tissues. The absolute protein quantitation of transporters and enzymes was performed by means of nano-LC-MS/MS with multiplexed SRM/multiple reactions monitoring as described previously (Uchida et al., 2015). The protein expression levels were determined as the amounts of trypsin-generated specific target peptides whose sequences had been selected based on in silico selection criteria (Kamiie et al., 2008). The SRM/multiple reactions monitoring transitions for the quantification of each peptide were set as reported previously (Miura et al., 2017) and are shown in Supplemental Table 1. The microdissected tissues were dissolved in denaturing buffer [7 M guanidium hydrochloride, 500 mM Tris-HCl (pH 8.5), 10 mM EDTA], and the proteins were S-carbamoylmethylated. The alkylated proteins were precipitated with a mixture of methanol and chloroform. The precipitates were dissolved in 6 M urea, and diluted with 100 mM Tris-HCl (pH 8.5). Enzymatic digestion with trypsin and lysylendopeptidase, liquid chromatography separation of peptides, and detection/-quantification of the target peptides were carried out as reported previously (Uchida et al., 2015). The individual expression amount of each peptide was determined as an average of three or four SRM transitions from three independent analyses.

The expression amount of each peptide was calculated as the mean ± S.D. of the average of individual expression amounts. In cases where no signal peak was detected, the amount of peptide in the sample was defined as under the limit of quantification. The limit of quantification (femtomoles per microgram protein) was calculated as the peptide amount expected to give a peak area count of 1000 in the chromatogram of samples, as reported previously (Uchida et al., 2015).

Liver Zonation Indices of Protein Expression in Mouse Liver Acinus. The liver zonation indices $Z(0)$ and $Z(100)$ were defined to show the relative distributions of protein expressions in the PP and PC vein regions, respectively. The $Z(0)$ index for each protein is defined as the protein level in the SR-101$^-$ PP vein region/[(the protein level in the SR-101$^-$ PP vein region + the protein level in the SR-101$^+$ PC vein region)/2]. The $Z(100)$ index for each protein is defined as the protein level in the SR-101$^+$ PC vein region/[(the protein level in the SR-101$^-$ PP vein region + the protein level in the SR-101$^+$ PC vein region)/2]. The values of $Z(0)$ and $Z(100)$ ranged from 0 to 2 [$0 \leq Z(0)$ or $Z(100) \leq 2$].

SR-101 Uptake by Mouse Oatp1a1- or Oarp2b1-Overexpressing HEK293 Cells. HEK293 cells transiently expressing Oatp1a1 and control HEK293 cells were generated by transfection of the open reading frame of Oatp1a1 inserted in the pcDNA5/FRT vector (Invitrogen, Carlsbad, CA) and the empty vector (mock), respectively. The open reading frame of mouse Oatp1a1 cDNA was obtained by reverse transcription polymerase chain reaction from mouse liver cDNA. The amino acid sequence translated from the Oatp1a1 cDNA is identical to that reported in the National Center for Biotechnology Information database (Gene Accession No. NM_013797). The transfection was performed using Lipofectamine 2000 and Opti-MEM I medium (Invitrogen) according to the manufacturer's protocol. Briefly, the cells were seeded at 90% confluence in 24-well plates using antibiotic-free medium. The complex of the vector and lipofectamine was incubated with the cells for 6 hours, and then the cells were cultured in normal culture medium for 24 hours. For the uptake study, the cells were washed with normal extracellular fluid buffer (122 mM NaCl, 25 mM NaHCO$_3$, 3 mM KCl, 0.4 mM K$_2$HPO$_4$, 10 mM glucose, 1.4 mM CaCl$_2$, 1.2 mM MgSO$_4$ and 10 mM HEPES, pH 7.4). Uptake was initiated by applying 200 μl normal extracellular fluid buffer containing 1 μM SR-101 at 37°C. After 20 minutes, the solution was removed to terminate uptake, and the cells were washed in ice-cold normal extracellular fluid buffer. Images were taken with a fluorescence microscope (Fluoview; Olympus, Tokyo, Japan). The cells were then homogenized in distilled water using a sonicator. The homogenate was centrifuged at 21,600g for 5 minutes at 4°C and the supernatant was collected. The cell-associated fluorescence was measured with a fluorescence detector (Fluoroscan Acent FL; Thermo Fisher Scientific, Waltham, MA). The accumulation of SR-101 in the cells was expressed as the cell-associated fluorescence per well. The method of SR-101 uptake by mouse Oatp2b1-overexpressing HEK293 cells is described in the Supplemental Material.

Statistical Analysis. An unpaired, two-tailed Student's t test was used to determine the significance of differences between two group mean values. One-way analysis of variance followed by the modified Fisher's least-squares difference method was used to assess the statistical significance of differences among the mean values of more than two groups. A value of $P < 0.01$ was considered statistically significant.

Results

Visualization of the PC Vein Regions in Mouse Liver with SR-101, and Zone-Specific Sampling by LMD. The zonated distribution of SR-101, a potent substrate of Oatps, was elucidated in frozen liver sections from mice intravenously injected with SR-101. As shown in Fig. 1A and Supplemental Fig. 1, A and B, there is an uneven distribution of SR-101 in the liver sections at the time points of 30 and 90 minutes, and regions that are strongly positive (SR-101$^+$) and either weakly positive or negative (SR-101$^-$) can be seen. The high magnification image at the time point of 90 minutes showed that SR-101 labeling was likely to be detected in the sinusoids and in part in the bile canaliculi (Supplemental Fig. 1C), suggesting that SR-101 was at least partly excreted into the bile. The following experiments were performed at the time point of 90 minutes. The uneven distribution of SR-101 in the liver sections was supported by the results of
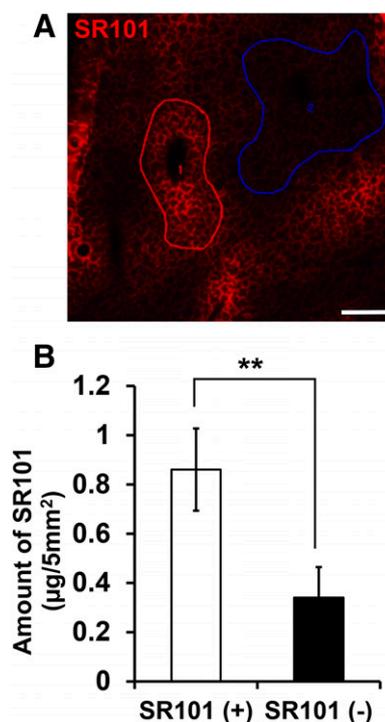
Fig. 1. Uneven distribution of SR-101 in the liver acinus of mice 90 minutes after intravenous administration of SR-101. (A) Representative fluorescence image of the liver. Areas 1 and 2 surrounded by red and blue lines are regions strongly positive for SR-101 (SR-101$^+$) and negative or weakly positive for SR-101 (SR-101$^-$), respectively. Scale bar, 100 μm. (B) Differences in SR-101 distribution amounts in the SR-101$^+$ and SR-101$^-$ regions. Each point represents the mean ± S.D. ($n = 3$) in three independent analyses. **$P < 0.01$, significantly different between the SR-101$^+$ and SR-101$^-$ regions.

LC-MS/MS-based quantification, which demonstrated that the amount of SR-101 in the SR-101$^+$ regions was over 2-fold greater than that in the SR-101$^-$ regions (Fig. 1B). QTAP analyses indicated that the protein level of glutamine synthetase, which exhibits selective distribution in hepatocytes in the PC vein region, was 480-fold greater in the SR-101$^+$ regions than the quantification limit in the SR-101$^-$ regions (Fig. 2A), whereas there was no significant difference in the expression levels of Na$^+$,K$^+$-ATPase, a plasma membrane marker, (Fig. 2B) and actin (Fig. 2C) between the regions. These results indicated that the SR-101$^+$ region corresponded to the PC vein region. There was no difference in the yields of the plasma membrane fraction and total proteins obtained from the SR-101$^+$ and SR-101$^-$ regions.

Comparison of Transporter/Receptor and Enzyme Protein Expression Levels in the SR-101$^+$ and SR-101$^-$ Regions of Mouse Liver. Supplemental Fig. 2 and Table 1 show comparisons of the protein expression levels of transporters/receptors in the SR-101$^+$ and SR-101$^-$ regions of mouse liver. There were statistically significant differences ($P < 0.01$) in the protein levels of Oatp1a1, organic cation transporter 1 (Oct1), and organic anion transporter 2 (Oat2) between the SR-101$^+$ and SR-101$^-$ regions. The protein levels of Oatp1a1 and Oct1 were 2.0- and 5.2-fold, respectively, greater in the SR-101$^+$ region, whereas the level of Oat2 was 2.4-fold greater in the SR-101$^-$ region. The protein level of Oatp1b2 was at least 1.9-fold greater in the SR-101$^+$ region compared with the value of the quantification limit in the SR-101$^-$ region. The level of Oatp2b1 was below the detection limit in both the SR-101$^+$ and SR-101$^-$ regions (Supplemental Table 2). In contrast, there were no significant differences in the levels of 4f2 cell-surface antigen heavy chain, equilibrative nucleoside transporter 1 (Ent1), Na$^+$-taurocholate cotransporting polypeptide, monocarboxylate transporter 1,
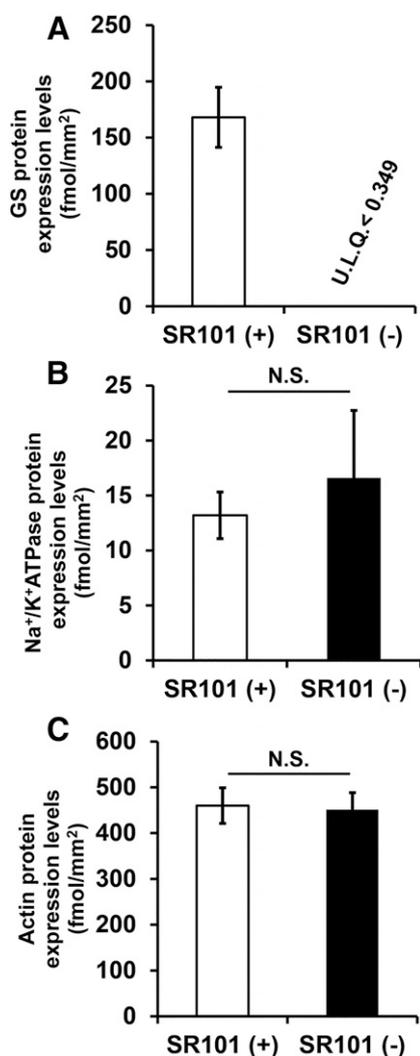
Fig. 2. Differences in the protein expression levels of glutamine synthetase (GS), a marker of hepatocytes in the PC vein region of the liver (A), Na$^+$,K$^+$-ATPase, a ubiquitously expressed marker of plasma membrane protein (B), and actin (C) in the SR-101$^+$ and SR-101$^-$ regions. Each column represents the mean $\pm$ S.D. ($n = 3$) in three independent analyses. N.S. represents no statistically significant difference. U.L.Q, under the limit of quantification.

Slc22a18, Abcb4, bile salt export pump, Mrp2, Mrp4, Mrp6, Abcg2/-breast cancer resistance protein, Abcg5, and neonatal Fc receptor between the SR-101$^+$ and SR-101$^-$ regions. Supplemental Fig. 2 and Table 1 show comparisons of the protein expression levels of metabolizing enzymes in the SR-101$^+$ and SR-101$^-$ regions of the liver. There was a statistically significant difference ($P < 0.01$) in the protein level of Cyp2e1, which was 54.5-fold greater in the SR-101$^+$ region. There were no statistically significant differences in the levels of Cyp2c29, Cyp2d22, Cyp3a11, Cyp8b1, Cyp51a1, Ugt1a1, Ugt1a9, Ugt2b36, and NADPH-cytochrome P450 reductase between the SR-101$^+$ and SR-101$^-$ regions, although Cyp2c29, Ugt1a1, and NADPH-cytochrome P450 reductase exhibited 2.3- to 3.2-fold greater average expression levels in the SR-101$^+$ region. The other molecules that were not detected in QTAP analyses (i.e., below the detection limit) are listed in Supplemental Table 2.

Liver Zonation Index Values of Protein Expressions in the PP and PC Vein Regions. Figures 3 and 4 summarize the liver zonation index values, where Z(0) and Z(100) represent the relative distributions of protein expressions in the PP and PC vein regions, respectively. The

Z(0) and Z(100) values of Cyp2e1, Oct1, Cyp2c29, Ugt1a1, NADPH-cytochrome P450 reductase, Oatp1a1, Cyp51a1, Slc22a18, Ent1, Cyp8b1, Ugt2b36, breast cancer resistance protein, monocarboxylate transporter 1, Mrp4, Mrp6, Ugt1a9, Abcb4, Mrp2, Na$^+$-taurocholate cotransporting polypeptide, Abcg5, Actin, Cyp2d22, 4f2 cell-surface antigen heavy chain, neonatal Fc receptor, and Cyp3a11 ranged from 0.036 to 0.990 and 1.96 to 1.01, respectively, in rank order. In contrast, the Z(0) and Z(100) values of Na,K-ATPase, bile salt export pump, and Oat2 ranged from 1.11 to 1.39 and 0.886 to 0.610 in rank order. The Z(0) and Z(100) values of Oat2, which exhibited the PP vein–predominant distribution (Table 1), were 1.39 and 0.610, respectively (Fig. 3), and the difference (δ) between the Z(0) and Z(100) showed the smallest value ($\delta = -0.780$). The Z(0) and Z(100) values of Oatp1a1, Oct1, and Cyp2e1, which exhibited the PC vein–predominant distribution (Table 1), were from 0.036 to 0.664 and 1.34 to 1.96, respectively (Figs. 3 and 4). The differences (δ) between the Z(0) and Z(100) of Oatp1a1 ($\delta = 0.672$), Oct1 ($\delta = 1.35$), and Cyp2e1 ($\delta = 1.93$) showed the greatest values among those tested. These results indicate that the liver zonation index could express the distinct zonation of the transporters/receptors and enzymes protein expression along the porto-central axis of the mouse liver acinus.

Comparison of Ribavirin Distribution in the SR-101$^+$ and SR-101$^-$ Regions of Mouse Liver. To examine whether the protein expression levels of Ent1, a major ribavirin uptake transporter in human hepatocytes (Fukuchi et al., 2010), correspond to the distribution of its transportable substrate, the distribution of ribavirin was quantified by LC-MS/MS in lysates of microdissected tissues derived from the SR-101$^+$ and SR-101$^-$ regions. Figure 5 shows that there was no significant difference in the amount of ribavirin present as the intact and phosphorylated forms in the SR-101$^+$ and SR-101$^-$ regions. Acid phosphatase treatment significantly increased the intact form of ribavirin in the samples derived from the SR-101$^+$ and SR-101$^-$ regions (Fig. 5). Ribavirin was mostly phosphorylated after it was taken up by the hepatocytes. These results indicated that the distribution of ribavirin was almost uniform, in accordance with the absence of statistically significant zonated expression of Ent1 (Supplemental Fig. 2; Table 1) in the mouse liver acinus.

SR-101 Uptake by Mouse Oatp1a1- and Oatp2b1-Overexpressing HEK293 Cells. Table 1 shows that the protein level of Oatp1a1 was 2.0-fold greater in the SR-101$^+$ region than in the SR-101$^-$ region, in accordance with the 2.0-fold greater distribution of SR-101 in the SR-101$^+$ region (Fig. 1B). The absolute expression amount of Oatp1a1 was approximately 7-fold or more greater than that of Oatp1b2 or Oatp2b1 (Supplemental Table 2; Table 1). This raised the possibility that Oatp1a1 contributes to the predominant distribution of SR-101 in the PC vein region, considering that previous reports have demonstrated that mouse Oatp1c1, an isoform of Oatps, mediates SR-101 transport (Schnell et al., 2015). Therefore, we first tested whether mouse Oatp1a1 mediates SR-101 transport by using Oatp1a1-overexpressing HEK293 cells (Oatp1a1/HEK293). As shown in Fig. 6, the SR-101 uptake was significantly greater in Oatp1a1/HEK293 cells than in the empty vector (mock)-transfected HEK293 cells. These results indicated that SR-101 is a substrate of mouse Oatp1a1. We next examined whether mouse Oatp2b1, another Oatp transporter, also mediates SR-101 transport by using Oatp2b1-overexpressing HEK293 cells (Oatp2b1/HEK293). As shown in Supplemental Fig. 3, there was a statistically significantly greater uptake of SR-101 in Oatp2b1/HEK293 cells than in the control HEK293 cells. These results indicated that SR-101 is also a substrate of mouse Oatp2b1.

Discussion

The present study demonstrates that sinusoidal membrane transporters such as Oatp1a1, Oatp1b2, and Oct1 are predominantly

TABLE 1

Protein expression levels of transporters/receptors and enzymes in SR-101$^+$ and SR-101$^-$ regions of mouse liver and liver zonation index values

Each value of the protein expression level represents the mean $\pm$ S.D. (n = 3) in three independent analyses. **P < 0.01, significantly different between SR-101$^+$ and SR-101$^-$ regions.

Alias	Protein Expression Levels (Mean $\pm$ S.D.)		Ratio of SR-101$^+$/SR-101$^-$
	SR-101$^+$	SR-101$^-$	
	fmol/mm^2	*fmol/mm^2*	
Slc transporter			
Slc3a2 (4F2hc)	0.917 $\pm$ 0.219	0.834 $\pm$ 0.016	1.10
Slc10a1 (Ntcp)	6.11 $\pm$ 1.42	4.74 $\pm$ 1.16	1.29
Slc16a1 (Mct1)	13.1 $\pm$ 3.0	9.00 $\pm$ 3.10	1.46
Slc21a1 (Oatp1a1)	30.2 $\pm$ 2.7	15.0 $\pm$ 4.8**	2.01
Slc21a10 (Oatp1b2)	4.30 $\pm$ 1.09	U.L.Q. < 2.25	>1.91
Slc22a1 (Oct1)	2.43 $\pm$ 0.37	0.470 $\pm$ 0.120**	5.17
Slc22a7 (Oat2)	0.343 $\pm$ 0.146	0.781 $\pm$ 0.113**	0.440
Slc22a18 (Slc22a18)	6.49 $\pm$ 1.02	3.57 $\pm$ 0.78	1.82
Slc29a1 (Ent1)	4.69 $\pm$ 0.07	2.76 $\pm$ 0.93	1.70
Abc transporter			
Abcb4 (Abcb4)	1.78 $\pm$ 0.39	1.38 $\pm$ 0.27	1.29
Abcb11 (Bsep)	2.48 $\pm$ 0.21	3.51 $\pm$ 0.70	0.710
Abcc2 (Mrp2)	2.17 $\pm$ 0.18	1.68 $\pm$ 0.17	1.29
Abcc4 (Mrp4)	0.227 $\pm$ 0.044	0.162 $\pm$ 0.011	1.40
Abcc6 (Mrp6)	3.04 $\pm$ 0.75	2.19 $\pm$ 0.89	1.39
Abcg2 (Bcrp)	4.16 $\pm$ 0.86	2.82 $\pm$ 1.05	1.48
Abcg5 (Abcg5)	0.939 $\pm$ 0.311	0.748 $\pm$ 0.142	1.26
Enzyme			
Cyp2c29 (Cyp2c29)	156 $\pm$ 74	49.0 $\pm$ 62.0	3.18
Cyp2d22 (Cyp2d22)	24.6 $\pm$ 5.7	22.3 $\pm$ 7.5	1.10
Cyp2e1 (Cyp2e1)	76.3 $\pm$ 25.9	1.40 $\pm$ 0.10**	54.5
Cyp3a11 (Cyp3a11)	68.1 $\pm$ 13.7	65.1 $\pm$ 15.7	1.05
Cyp8b1 (Cyp8b1)	2.58 $\pm$ 0.52	1.67 $\pm$ 0.94	1.54
Cyp51a1 (Cyp51a1)	6.62 $\pm$ 0.41	3.48 $\pm$ 1.19	1.90
Ugt1a1 (Ugt1a1)	45.4 $\pm$ 10.2	19.4 $\pm$ 5.1	2.34
Ugt1a9 (Ugt1a9)	69.4 $\pm$ 22.3	52.1 $\pm$ 16.7	1.33
Ugt2b36 (Ugt2b36)	63.2 $\pm$ 6.4	42.4 $\pm$ 13.8	1.49
Por (NADPH-CPR)	37.7 $\pm$ 9.8	16.1 $\pm$ 3.1	2.34
Other			
Fcgrt (FcRn)	4.26 $\pm$ 0.59	3.88 $\pm$ 0.54	1.10
Glul (GS)	168 $\pm$ 31	U.L.Q. < 0.349	>481
Atp1a1-3 (Na,K-ATPase)	13.2 $\pm$ 0.40	16.6 $\pm$ 6.4	0.795
Actin	460 $\pm$ 36	451 $\pm$ 34	1.02

Abc, ATP-binding cassette; Bcrp, breast cancer resistance protein; Bsep, bile salt export pump; CPR, cytochrome P450 reductase; 4F2hc, 4f2 cell-surface antigen heavy chain; FcRn, neonatal Fc receptor; GS, glutamine synthetase; Mct1, monocarboxylate transporter 1; Ntcp, Na$^+$-taurocholate cotransporting polypeptide; Slc, solute carrier; U.L.Q., under the limit of quantification.

expressed in the PC vein region, while Oat2 is predominantly in the PP vein region of mouse liver acinus, based on the liver zonation index of the protein distributions of transporters and enzymes.

There is increasing evidence that Oatp1a1, Oatp1b2, Oct1, and Ent1 contribute to drug transport at the sinusoidal plasma membrane of hepatocytes. Our results here suggest that the PC vein region–predominant distribution of SR-101 can be explained by the at least 7-fold greater expression level of Oatp1a1 than that of Oatp1b2 and Oatp2b1 in the SR-101$^+$-PC vein region and the Oatp1a1-mediated transport of SR-101. Since we observed Oatp2b1-mediated SR-101 uptake, there is also a possibility that Oatp1b2, another Oatp transporter, could mediate SR-101 transport in part and thus contribute to the PC vein region–predominant distribution of SR-101. It would be intriguing in future studies to examine the contributions of Oatp1a1 and Oatp1b2 to the zonated distribution of SR-101 using gene-knockout mice. It would also be interesting to examine whether a lower-affinity transport system for SR-101 in the PP or PC vein regions may be involved in the region-specific distribution by using a bolus administration of SR-101 with a higher dose. On the other hand, the absence of a significant difference of Ent1 expression in the PP and PC vein regions is in good agreement with the almost homogeneous distribution of ribavirin, an Ent1 substrate (Fukuchi et al., 2010). These findings are consistent with the idea that

sinusoidal membrane transport is a key determinant of the zonated distribution of drugs in the liver. The bile excretion of the angiotensin-converting enzyme inhibitor temocaprilat, an active metabolite of temocapril that is rapidly formed by hydrogenation after oral administration, involves Oatp1a1-mediated uptake at the sinusoidal membrane (Ishizuka et al., 1998), followed by Mrp2-mediated efflux transport (Ishizuka et al., 1997) at the canalicular membrane of hepatocytes. The predominant expression of Oatp1a1 in the PC vein region and the almost homogenous distribution of Mrp2 in the PP and PC vein regions suggest that the sinusoidal uptake of temocaprilat contributes to its predominant distribution in the PC vein region. The previous findings of a marked decrease in the biliary excretion of temocaprilat and pravastatin after zone 3 injury (Takikawa et al., 2001) could be explained by the present observation of predominant distribution of Oapt1a1 in the PC vein region. The protein expression level of Oatp1b2, the functional homolog of human OATP1B1 and OATP1B3 (Zaher et al., 2008), in the PC vein region is at least 2-fold greater than the under the limit of quantification value in the PP vein region. Since studies with Oatp1b2 knock-out mice showed that Oatp1b2 plays a significant role in the hepatobiliary disposition of lovastatin (Chen et al., 2008), an inhibitor of hydroxymethylglutaryl-CoA reductase, which catalyzes the rate-limiting step in cholesterol biosynthesis, it can be anticipated that
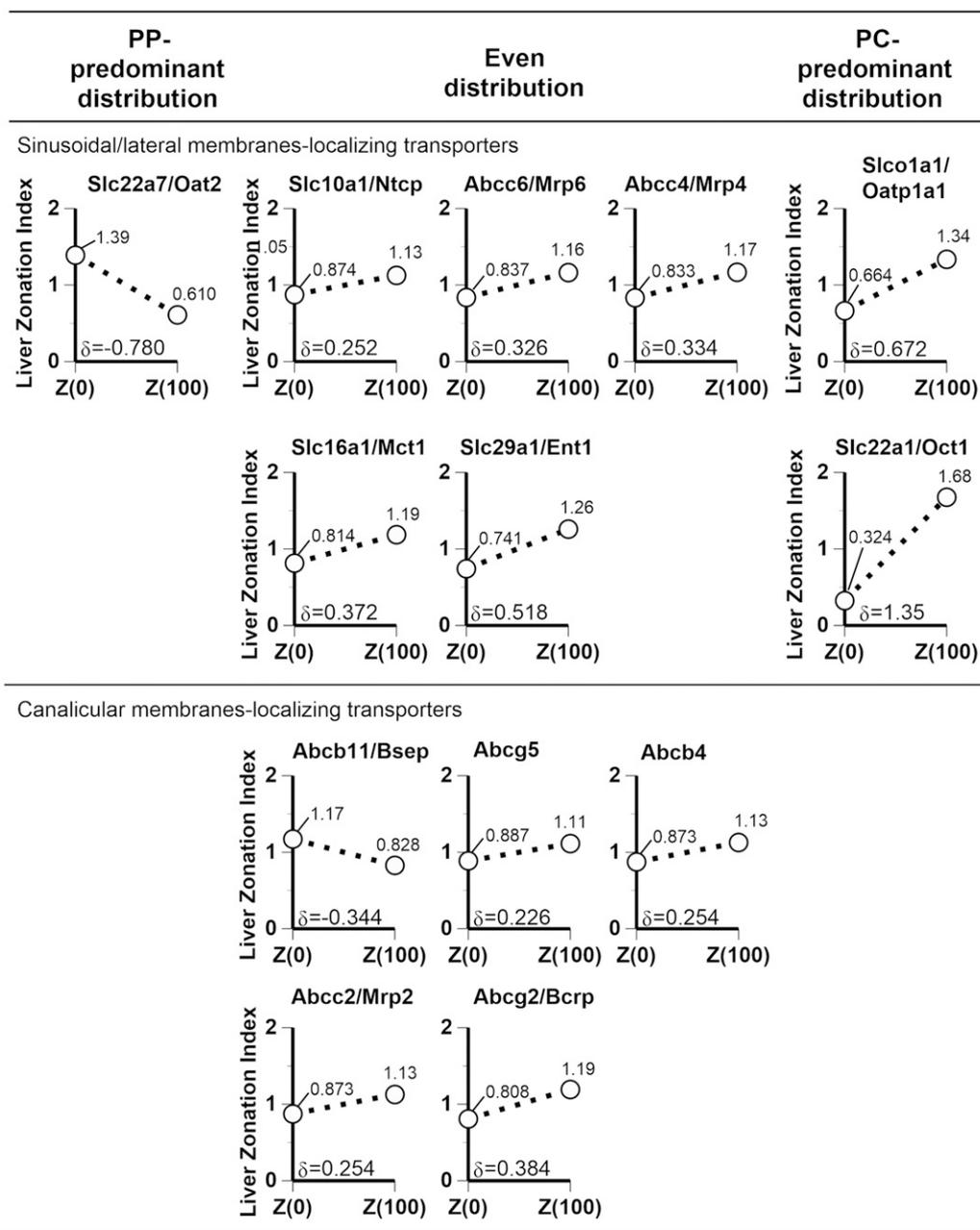
Fig. 3. Liver zonation index values of transporter protein distributions. The liver zonation indexes Z(0) and Z(100) for each protein were plotted based on the data shown in Table 1. The values of Z(0) and Z(100) were calculated as shown in *Materials and Methods*. The differences (δ) between the values of Z(0) and Z(100) are indicated in each graph.

lovastatin would be distributed predominantly in the PC vein region. In contrast, predominant protein distribution of hydroxymethylglutaryl-CoA reductase in the PP vein region of the liver has been found in normal and hydroxymethylglutaryl-CoA reductase inhibitor (mevino-lin)–treated male rats fed standard laboratory chow (Singer et al., 1984). This is a case where the predominant region of transporter protein expression is different from that of the drug target expression in the liver. A similar situation exists for the PC vein–predominant expression of Oct1, which is consistent with the previous immunohistochemical result for Oct1 in rat liver (Meyer-Wentrup et al., 1998). Oct1 mediates hepatic uptake of several prescription drugs, most notably the antidiabetic agent metformin (Shu et al., 2007). On the other hand, the functional activity of AMP-activated kinase, the target of metformin, is greater in the PP vein region than in the PC vein region (Witters et al., 1994). Therefore,

evaluation of drug targeting to hepatocytes needs to take into account the zonated expressions of both transporters and the target molecules in the liver.

It has been proposed that Oct1 works in concert with drug-metabolizing enzymes in detoxification pathways in the liver (Zhang et al., 2006). In support of this proposal, the present results indicate a greater expression level of Cyp2e1 in the PC vein region and a tendency for PC vein region–predominant distribution of Cyp2c29 and Ugt1a1. The PC vein–predominant distributions of Cyp enzymes are consistent with previous reports on the expression of Cyp2c29 and Cyp2e1 at the protein and transcript levels (Braeuning et al., 2006). The greater expression of Ugt1a1 is also in good agreement with the PC vein–dominant total activity of UDP-glucuronyl transferase (el Mouelhi and Kauffman, 1986). Thus, consideration of the zonated expressions of
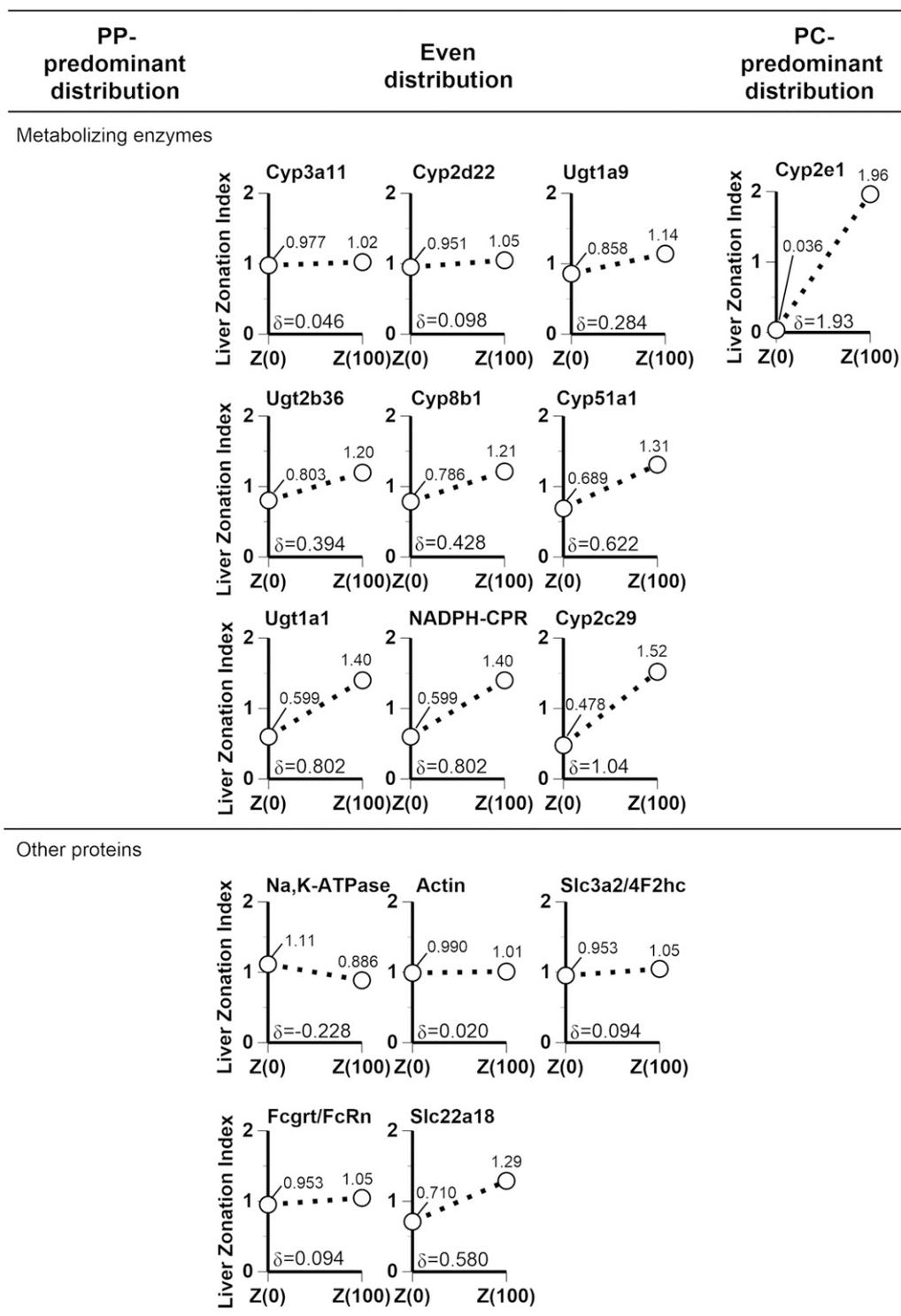
Fig. 4. Liver zonation index values of metabolizing enzyme and other protein distributions. The liver zonation indexes Z(0) and Z(100) for each protein were plotted based on the data shown in Table 1. The values of Z(0) and Z(100) were calculated as shown in *Materials and Methods*. The differences (δ) between the values of Z(0) and Z(100) are indicated in each graph.

uptake transporters and metabolizing enzymes together may lead to better predictions of clearance, especially in the case of drugs with limited liver permeability.

The predominant protein expression of Oat2 in the PP vein region is not consistent with previous mRNA quantification results suggesting no difference in the transcript levels of Oat2 in the PC and PP vein regions (Fork et al., 2011). This discrepancy could be explained by our previous

result showing that there is no correlation between mRNA and protein amounts of plasma membrane transporters in human liver (Ohtsuki et al., 2012). Functional analyses have demonstrated that Oat2 on the sinusoidal membrane of hepatocytes mediates the efflux transport of glutamate from hepatocytes in rats (Fork et al., 2011). This process may be involved in spatial regulation of glutamate metabolism in the liver, i.e., the efflux of glutamate from hepatocytes in the PP vein
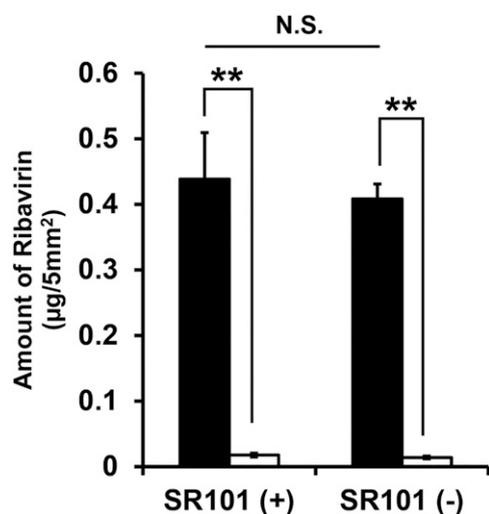
Fig. 5. Differences in ribavirin distribution amounts in the SR-101$^+$ and SR-101$^-$ regions of mice 90 minutes after intravenous administration of both SR-101 and ribavirin. The amount of ribavirin was determined in the microdissected tissues with (closed column) or without (open column) acid phosphatase treatment. Each column represents the mean $\pm$ S.D. ($n = 3$) in three independent analyses. **$P < 0.01$, significantly different between the indicated groups. N.S. represents no statistically significant difference between the SR-101$^+$ and SR-101$^-$ groups.

Fig. 6. Mouse Oatp1a1 mediates SR-101 uptake. (A) Representative fluorescence images of SR-101 in mock-transfected HEK293 cells (Mock/HEK293; image A1) and mouse Oatp1a1-overexpressing HEK293 cells (Oatp1a1/HEK293; image A2). Scale bar, 50 μm. (B) Comparison of the SR-101 uptake amounts in Mock/HEK293 cells (open column) and Oatp1a1/HEK293 cells (closed column). Each column represents the mean $\pm$ S.E.M. ($n = 3$). **$P < 0.01$, significantly different between Oatp1a1/HEK293 and Mock/HEK293 cells.

region followed by glutamine synthesis from glutamate in hepatocytes of the PC vein region, where expression of glutamine synthetase is concentrated.

Hepatic drug transport and metabolizing activities have been evaluated by using in vitro human hepatocytes during drug development (Houston et al., 2012; Godoy et al., 2013), with the assumption that hepatocytes exhibit uniform profiles of drug transport and metabolism activities. The present findings on the PP and PC vein region–specific protein expression amounts of transporters and metabolizing enzymes therefore have implications for selecting the source of hepatocytes for in vitro assays, and also suggest that it may be necessary to normalize drug transport and enzymatic activities to enable more precise simulation and modeling studies aimed at in vivo prediction. Furthermore, there have been increasing numbers of reports on tissue-level kinetic modeling of endogenous and xenobiotic metabolism in the liver based on the metabolic zonation concept (Lerapetritou et al., 2009). Ohno et al. (2008) reported results on single-hepatocyte-based lobular models of ammonia metabolism that incorporate liver zone-specific gene expression of major enzyme transporters. Knowledge of the region-specific absolute protein amounts and the liver zonation index of transporters/enzymes introduced in the present study would be essential to construct reliable in silico liver distribution and clearance in pharmacokinetic tube and tank-in series models.

Previous studies of the zonated expressions of transporters and metabolizing enzymes by means of immunohistochemistry (Micuda et al., 2008) and by reverse transcription polymerase chain reaction of isolated PP and PC vein hepatocytes obtained by ante- or retrograde perfusion with digitonin/collagenase (Baier et al., 2006) as summarized in Supplemental Table 3 have revealed some discrepancies. For example, the present study indicates 2-fold greater expression protein levels of Oatp1a1 in the PC vein region of mouse liver, whereas previous reports demonstrate the homogenous distribution of Oatp1a1 in the PP and PC vein regions of rat liver (Abu-Zahra et al., 2000; Baier et al., 2006). These results may be at least partly due to differences in the selected regions of liver tissue or differences in cell sampling by perfusion-based hepatocyte isolation. In the present study, we collected PP and PC vein region–predominant hepatocytes by
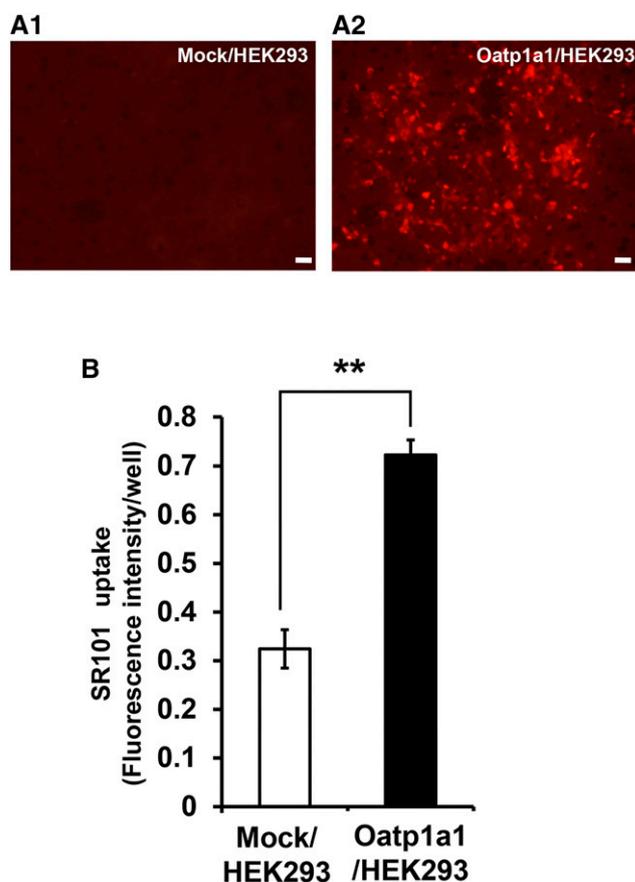
fluorescence-guided LMD, based on the distribution of SR-101 in the liver. Therefore, the present results have the advantage of directly clarifying the relationship between the protein expression levels and the zonated substrate disposition. As shown in Supplemental Fig. 4, the expression levels of transporters normalized by the level of 4f2 cell-surface antigen heavy chain, which showed homogenous protein expression in the PP and PC vein regions in the present study, are consistent with those obtained in plasma membrane fractions of total mouse liver (Miura et al., 2017) within differences of less than 2-fold, except for Oatp1a1, bile salt export pump, and Abcb4. This result suggests that the amounts determined with LMD-generated samples are broadly consistent with those obtained using wet liver tissues. However, the level of Oatp1a1, which exhibits PC vein region–dominant expression, tends to be underestimated in the plasma membrane fractions of mouse liver. Considering that Mrp6 and Abcb4 did not show zonated expression in the present study, the intracellular localization as well as the plasma membrane localization could have influenced the overestimation of the expression levels in the LMD-generating samples. Furthermore, it has been reported that total taurocholate uptake decreased during monolayer cultivation of hepatocytes, and the zonal differences observed in freshly isolated cells in suspension disappeared (Ugele and Gebhardt, 2003). Therefore, in vivo zonated tissue sample preparation and quantification of transporter protein levels should provide a superior basis for estimating the liver region–specific distribution of drugs.

In conclusion, the present study has demonstrated the zonated protein expression profiles of major transporters and metabolizing enzymes in mouse liver acinus. This information should be helpful in developing liver-targeting drugs and for establishing predictive models of the hepatic clearance of drugs.

Authorship Contributions

Participated in research design: Tachikawa, Sumiyoshiya, Saigusa, Watanabe, Uchida, Terasaki.

Conducted experiments: Tachikawa, Sumiyoshiya, Saigusa, Sasaki.

Contributed new reagents or analytic tools: Watanabe, Uchida, Terasaki.

Performed data analysis: Tachikawa, Sumiyoshiya, Saigusa, Sasaki.

Wrote or contributed to the writing of the manuscript: Tachikawa, Sumiyoshiya, Saigusa, Sasaki, Watanabe, Uchida, Terasaki.

References

Abu-Zahra TN, Wolkoff AW, Kim RB, and Pang KS (2000) Uptake of enalapril and expression of organic anion transporting polypeptide 1 in zonal, isolated rat hepatocytes. *Drug Metab Dispos* **28**:801–806.

Aiso M, Takikawa H, and Yamanaka M (2000) Biliary excretion of bile acids and organic anions in zone 1- and zone 3-injured rats. *Liver* **20**:38–44.

Baier PK, Hempel S, Waldvogel B, and Baumgartner U (2006) Zonation of hepatic bile salt transporters. *Dig Dis Sci* **51**:587–593.

Braeuning A, Ittrich C, Köhle C, Hailfinger S, Bonin M, Buchmann A, and Schwarz M (2006) Differential gene expression in periportal and perivenous mouse hepatocytes. *FEBS J* **273**:5051–5061.

Chen C, Stock JL, Liu X, Shi J, Van Deusen JW, DiMattia DA, Dullea RG, and de Morais SM (2008) Utility of a novel Oatp1b2 knockout mouse model for evaluating the role of Oatp1b2 in the hepatic uptake of model compounds. *Drug Metab Dispos* **36**:1840–1845.

Ellis LC, Hawksworth GM, and Weaver RJ (2013) ATP-dependent transport of statins by human and rat MRP2/Mrp2. *Toxicol Appl Pharmacol* **269**:187–194.

el Mouelhi M and Kauffman FC (1986) Sublobular distribution of transferases and hydrolases associated with glucuronide, sulfate and glutathione conjugation in human liver. *Hepatology* **6**:450–456.

Fork C, Bauer T, Golz S, Geerts A, Weiland J, Del Turco D, Schömig E, and Gründemann D (2011) OAT2 catalyses efflux of glutamate and uptake of orotic acid. *Biochem J* **436**:305–312.

Fukuchi Y, Furihata T, Hashizume M, Iikura M, and Chiba K (2010) Characterization of ribavirin uptake systems in human hepatocytes. *J Hepatol* **52**:486–492.

Godoy P, Hewitt NJ, Albrecht U, Andersen ME, Ansari N, Bhattacharya S, Bode JG, Bolleyn J, Borner C, Böttger J, et al. (2013) Recent advances in 2D and 3D in vitro systems using primary hepatocytes, alternative hepatocyte sources and non-parenchymal liver cells and their use in investigating mechanisms of hepatotoxicity, cell signaling and ADME. *Arch Toxicol* **87**:1315–1530.

Groothuis GM, Hardonk MJ, Keulemans KP, Nieuwenhuis P, and Meijer DK (1982) Autoradiographic and kinetic demonstration of acinar heterogeneity of taurocholate transport. *Am J Physiol* **243**:G455–G462.

Gumucio JJ, Balabaud C, Miller DL, DeMason LJ, Appelman HD, Stoecker TJ, and Franzblau DR (1978) Bile secretion and liver cell heterogeneity in the rat. *J Lab Clin Med* **91**:350–362.

Houston JB, Rowland-Yeo K, and Zanelli U (2012) Evaluation of the novel in vitro systems for hepatic drug clearance and assessment of their predictive utility. *Toxicol In Vitro* **26**:1265–1271.

Ishizuka H, Konno K, Naganuma H, Nishimura K, Kouzuki H, Suzuki H, Stieger B, Meier PJ, and Sugiyama Y (1998) Transport of temocaprilat into rat hepatocytes: role of organic anion transporting polypeptide. *J Pharmacol Exp Ther* **287**:37–42.

Ishizuka H, Konno K, Naganuma H, Sasahara K, Kawahara Y, Niinuma K, Suzuki H, and Sugiyama Y (1997) Temocaprilat, a novel angiotensin-converting enzyme inhibitor, is excreted in bile via an ATP-dependent active transporter (cMOAT) that is deficient in Eisai hyperbilirubinemic mutant rats (EHBR). *J Pharmacol Exp Ther* **280**:1304–1311.

Jones AL, Hradek GT, Renston RH, Wong KY, Karlaganis G, and Paumgartner G (1980) Autoradiographic evidence for hepatic lobular concentration gradient of bile acid derivative. *Am J Physiol* **238**:G233–G237.

Kamiie J, Ohtsuki S, Iwase R, Ohmine K, Katsukura Y, Yanai K, Sekine Y, Uchida Y, Ito S, and Terasaki T (2008) Quantitative atlas of membrane transporter proteins: development and application of a highly sensitive simultaneous LC/MS/MS method combined with novel in-silico peptide selection criteria. *Pharm Res* **25**:1469–1483.

Katz NR (1992) Metabolic heterogeneity of hepatocytes across the liver acinus. *J Nutr* **122** (Suppl 3):843–849.

Kawakami H, Ohtsuki S, Kamiie J, Suzuki T, Abe T, and Terasaki T (2011) Simultaneous absolute quantification of 11 cytochrome P450 isoforms in human liver microsomes by liquid chromatography tandem mass spectrometry with in silico target peptide selection. *J Pharm Sci* **100**:341–352.

Lerapetritou MG, Georgopoulos PG, Roth CM, and Androulakis LP (2009) Tissue-level modeling of xenobiotic metabolism in liver: an emerging tool for enabling clinical translational research. *Clin Transl Sci* **2**:228–237.

Meyer-Wentrup F, Karbach U, Gorboulev V, Arndt P, and Koepsell H (1998) Membrane localization of the electrogenic cation transporter rOCT1 in rat liver. *Biochem Biophys Res Commun* **248**:673–678.

Micuda S, Fuksa L, Brcakova E, Osterreicher J, Cermanova J, Cibicek N, Mokry J, Staud F, and Martinkova J (2008) Zonation of multidrug resistance-associated protein 2 in rat liver after induction with dexamethasone. *J Gastroenterol Hepatol* **23**:e225–e230.

Miura T, Tachikawa M, Ohtsuka H, Fukase K, Nakayama S, Sakata N, Motoi F, Naitoh T, Katayose Y, Uchida Y, et al. (2017) Application of quantitative targeted absolute proteomics to profile protein expression changes of hepatic transporters and metabolizing enzymes during cholic acid-promoted liver regeneration. *J Pharm Sci* **106**:2499–2508.

Ninomiya M, Ito K, Hiramatsu R, and Horie T (2006) Functional analysis of mouse and monkey multidrug resistance-associated protein 2 (Mrp2). *Drug Metab Dispos* **34**:2056–2063.

Ohno H, Naito Y, Nakajima H, and Tomita M (2008) Construction of a biological tissue model based on a single-cell model: a computer simulation of metabolic heterogeneity in the liver lobule. *Artif Life* **14**:3–28.

Ohtsuki S, Schaefer O, Kawakami H, Inoue T, Liehner S, Saito A, Ishiguro N, Kishimoto W, Ludwig-Schwellinger E, Ebner T, et al. (2012) Simultaneous absolute protein quantification of transporters, cytochromes P450, and UDP-glucuronosyltransferases as a novel approach for the characterization of individual human liver: comparison with mRNA levels and activities. *Drug Metab Dispos* **40**:83–92.

Ohtsuki S, Uchida Y, Kubo Y, and Terasaki T (2011) Quantitative targeted absolute proteomics-based ADME research as a new path to drug discovery and development: methodology, advantages, strategy, and prospects. *J Pharm Sci* **100**:3547–3559.

Oinonen T and Lindros KO (1998) Zonation of hepatic cytochrome P-450 expression and regulation. *Biochem J* **329**:17–35.

Sakamoto A, Suzuki S, Matsumaru T, Yamamura N, Uchida Y, Tachikawa M, and Terasaki T (2016) Correlation of organic cation/carnitine transporter 1 and multidrug resistance-associated protein 1 transport activities with protein expression levels in primary cultured human tracheal, bronchial, and alveolar epithelial cells. *J Pharm Sci* **105**:876–883.

Sasamoto T, Sano N, and Takikawa H (2006) Biliary excretion of sulfated bile acids and organic anions in zone 1- and zone 3-injured rats. *J Gastroenterol Hepatol* **21**:26–31.

Schnell C, Shahmoradi A, Wichert SP, Mayerl S, Hagos Y, Heuer H, Rossner MJ, and Hülsmann S (2015) The multispecific thyroid hormone transporter OATP1C1 mediates cell-specific sulforhodamine 101-labeling of hippocampal astrocytes. *Brain Struct Funct* **220**:193–203.

Shu Y, Sheardown SA, Brown C, Owen RP, Zhang S, Castro RA, Ianculescu AG, Yue L, Lo JC, Burchard EG, et al. (2007) Effect of genetic variation in the organic cation transporter 1 (OCT1) on metformin action. *J Clin Invest* **117**:1422–1431.

Singer II, Kawka DW, Kazazis DM, Alberts AW, Chen JS, Huff JW, and Ness GC (1984) Hydroxymethylglutaryl-coenzyme A reductase-containing hepatocytes are distributed periportally in normal and mevinolin-treated rat livers. *Proc Natl Acad Sci USA* **81**:5556–5560.

Takai N and Tanaka Y (2015) Imaging of drug and metabolite distribution by MS: case studies. *Bioanalysis* **7**:2639–2648.

Takikawa H, Sano N, Onishi T, Ohashi M, Hasegawa Y, and Nishikawa K (2001) Biliary excretion of temocapril in zone 1- and zone 3-injured rat. *Hepatol Res* **20**:216–220.

Tokui T, Nakai D, Nakagomi R, Yawo H, Abe T, and Sugiyama Y (1999) Pravastatin, an HMG-CoA reductase inhibitor, is transported by rat organic anion transporting polypeptide, oatp2. *Pharm Res* **16**:904–908.

Uchida Y, Zhang Z, Tachikawa M, and Terasaki T (2015) Quantitative targeted absolute proteomics of rat blood-cerebrospinal fluid barrier transporters: comparison with a human specimen. *J Neurochem* **134**:1104–1115.

Ugele B and Gebhardt R (2003) Heterogeneity of rat liver parenchyma in taurocholate uptake. *Hepatol Res* **27**:238–247.

Witters LA, Gao G, Kemp BE, and Quistorff B (1994) Hepatic 5′-AMP-activated protein kinase: zonal distribution and relationship to acetyl-CoA carboxylase activity in varying nutritional states. *Arch Biochem Biophys* **308**:413–419.

Zaher H, Meyer zu Schwabedissen HE, Tirona RG, Cox ML, Obert LA, Agrawal N, Palandra J, Stock JL, Kim RB, and Ware JA (2008) Targeted disruption of murine organic anion-transporting polypeptide 1b2 (Oatp1b2/Slco1b2) significantly alters disposition of prototypical drug substrates pravastatin and rifampin. *Mol Pharmacol* **74**:320–329.

Zhang L, Strong JM, Qiu W, Lesko LJ, and Huang SM (2006) Scientific perspectives on drug transporters and their role in drug interactions. *Mol Pharm* **3**:62–69.

Address correspondence to: Dr. Masanori Tachikawa, Membrane Transport and Drug Targeting Laboratory, Graduate School of Pharmaceutical Sciences, Tohoku University, 6-3 Aramaki, Aoba, Sendai 980-8578, Japan. E-mail: tachik-dds@umin.ac.jp